Egyptian Journal Of

GENETICS AND CYTOLOGY

INTERNATIONAL JOURNAL DEVOTED TO GENETICAL AND CYTOLOGICAL SCIENCES

Published by

THE EGYPTIAN SOCIETY OF GENETICS

Volume 54 **January 2025** **No. 1**

ISOLATION, IDENTIFICATION AND BIOCONTROL POTENTIAL OF NATIVE SOIL-DERIVED *Trichoderma* spp.

NEHAL ATTA, ABDELMEGID I FAHMI*, KHALID S. ABDEL-LATEIF, HESHAM H. NAGATY AND ENAS M. ABD EL-GHANY

Genetics Department, Faculty of Agriculture, Menoufia University, Shibin El-Kom, Egypt

*Corresponding author: Abdelmegid I Fahmi, abdelmageed.fahmy@agr.menofia.edu.eg

Keywords: biocontrol agents, phytopathogenic fungi, *Trichoderma* spp., phylogenetic analysis, anti-fungal activity.

Trichoderma is considered one of the most efficient biocontrol agents (Yao *et al*. 2023). Its robust reproductive capacity, stress tolerance, ability to efficiently use nutrients to modify the rhizosphere, aggression towards phytopathogenic fungus, ability to promote plant growth, induction of defensive mechanisms, and provision of numerous secondary metabolites (Kredics *et al*. 2024), enzymes (Elad 2000), and pathogenesis-related (PR) proteins (Yadav *et al*. 2021) all contribute to its unique characteristics. Because of these characteristics, Various strains of *Trichoderma* represent around 90% of all fungal biological control agents, especially diseases caused by *Rhizoctonia solani* and *Macrophomina phaseolina*, which considered highly destructive soil-borne pathogenic fungi. Native *Trichoderma* strains indigenous to the crop rhizosphere are likely superior in serving as biocontrol agents. This is due to their proximity to plant roots, which

increases the likelihood of establishing endophytic relationships. *Trichoderma* uses direct and indirect techniques, such as antibiosis, nutritional competition, and mycoparasitism, to combat pathogenic fungal strains (Lahlali *et al*. 2022). During direct mycoparasitism, *Trichoderma* either generates hook- and appressorium-like structures or coils around pathogenic fungal hyphae (Ghasemi *et al*. 2019). The subsequent phase involves enzymatic and mechanical penetration of the pathogen by *Trichoderma*. These enzymes are primarily chitinases and other enzymes, such as β-glucanases and proteases. Thus, *Trichoderma* effectively breaks down the cell wall components of pathogens. In antibiosis, *Trichoderma* produces volatile and nonvolatile compounds that either cause growth inhibition or induce changes in phytopathogens (El-Hasan *et al*. 2022). Indirect mechanisms include plant growth promotion, nutritional and space competition, and plant systemic resistance induction (Elhamouly *et al*. 2022). One major antagonistic mechanism that *Trichoderma* spp. is known to exhibit is mycoparasitism. (Mukherjee *et al*. 2022). Thus, it is believed that *Trichoderma* chitinolytic strains are among the most efficient biocontrol agents for various diseases in plants. (Yadav *et al*. 2021). The extensive distribution of *Trichoderma* in various ecological habitats has been crucial in influencing the evolution of this species, promoting substantial genetic variation. Therefore, *Trichoderma* species must be accurately identified and characterized to effectively maximize their potential in specific applications. Additionally, species identification must be accurate because of the similar morphology and complex taxonomy of *Trichoderma* (Hermosa *et al*. 2000). Morphology alone is not sufficient for accurate identification of *Trichoderma* species, especially when dealing with genetically diverse groups such as the *T. harzianum* or *T. viride* complex, which are characterized by variable morphology. Many researchers have identified inaccuracies in *Trichoderma* taxonomy using only morphological characters, confirming the necessity of phylogenies based on sequencing data. Analysis methods based on DNA have been developed to construct a better taxonomy of the *Trichoderma* genus. One of significant and unique techniques for identifying different species is DNA barcoding, which mainly uses the nuclear rRNA ITS region (Raja *et al*. 2017). At the present time, more than 400 species have legitimate names in Mycobank, and most of them have been described based on phylogenetic analyses of DNA sequences. This study aims to identify isolates accurately at the species level via DNA sequence analysis of ITS region within the current taxonomic framework. Additionally, the present investigation aims to evaluate the isolates' potential to function as biological control microorganisms against two of most devastating soil-borne pathogenic fungi "*Rhizoctonia solani* and *Macrophomina phaseolina*", which are recognized for causing substantial crop losses globally (Zhao *et al*. 2024).

MATERIALS AND METHODS

Trichoderma isolation and morphological characterization

Representative soil samples from each site containing different cultivated crops were collected from nine governorates in Egypt (Cairo, Giza, Qalyubia, Dakahlia, Gharbia, Damietta, Beheira, Menoufia, and Kafr El-Sheikh) (Fig. 1). *Trichoderma* isolation and morphological characterization were conducted in accordance with the description provided by Fahmi *et al*. (2016).

Molecular identification of *Trichoderma*

DNA was extracted *via* the Riffiani *et al*. (2021) technique Amplification procedure using PCR technique was applied to the complete fragment of Internal Transcribed Spacers (ITS 1 and 2, and 5.8S rRNA) (Table 1).

PCR amplification was conducted in a 50 µL reaction system comprising 25 µL of PCR master mix (Promega Corp., Madison, Wisconsin), 1 µL of each primer, 1 µL DNA template, and 22 µL of ddH_2O. The PCR program amplification was set up as described in Table (2).

After that, the PCR products undergo purification and sequencing bidirectionally by Beijing Liuhe BGI Gene Technology Co., Ltd. (Beijing, China) via Sanger sequencing. The sequences of ITS locus were checked for quality, trimmed, and assembled into reference sequences to generate consensus sequences *via* Sequencher® 5.4.6 software from Gene Codes Corporation, Ann Arbor, MI, USA (http://www.genecodes.com). BLAST analysis was performed for each gene locus separately to authenticate the identification of the obtained isolates. The consensus sequences were submitted to GenBank to obtain accession numbers.

Phylogenetic analysis

A BLAST search using the obtained ITS gene sequences in the NCBI GenBank database was conducted. The ITS gene sequences of the isolates were retrieved from GenBank and aligned via the MUSCLE program (Edgar 2004), and the resulting alignment was further adjusted via BioEdit 7.2.5 software (Hall *et al*. 2011). For phylogenetic and molecular evolutionary analyses, the maximum likelihood (ML) method was employed via MEGA version 11 (Tamura *et al*. 2021), with 1,000 bootstrap replicates used to assess statistical support. Finally, the obtained ML tree was illustrated via Figtree v1.4.4 software (http://tree.bio.ed.ac.uk/software/figtree/), which provides a distinct depiction of the evolutionary connections among the isolates.

Antagonistic assay

A dual culture assay was employed to assess the potential antagonistic activity of 31 *Trichoderma* spp. isolates against *R. solani* or *M. phaseolina* (Dhingra and Sinclair 1995) that were provided by Agricultural Botany Department, Faculty of

Agriculture, Menoufia University. The radial growth inhibition percentage of the pathogen was determined via the following equation:(%) Inhibition in Mycelial Growth $=\frac{D1-D2}{D1} \times 100$

Where **D1 =** pathogen radial growth in the control, while **D2 =** pathogen radial growth in dual culture (with the antagonist).

Finally, the antagonistic types of *Trichoderma* isolates were identified in accordance with Fahmi *et al*. (2016).

Data analysis

Analyses of the average diameter of the pigmented region on agar medium, the concentration of released NAGA, and the inhibition percentage in the radial growth of different pathogenic fungi were carried out *via* ANOVA. Duncan's multiple range test ($P < 0.05$) was used to calculate differences via the CoStat statistical program version 6.311 copyright 1998--202008 Cohort Software. 798 Lighthouse Ave. PMB 320, Monterey, CA, 93940, USA.

RESULTS AND DISCUSSION

***Trichoderma* isolates' morphological identification**

Thirty-one native *Trichoderma* isolates were obtained from 98 samples, with an isolation rate of 30%, from different agroclimatic zones of central Egypt. Table (3) and Fig. (2) show the macroscopic characteristics of the colonies, which generally differ in shape from circular to serrate and vary in color from yellow, yellowish-white, and pale to dark green. The pigmentation varied in color from white to creamy, yellow, light amber, and amber, and concentric ring numbers ranged from one to three defined rings. The growth edges differed from smooth to wavey edges.

Concerning the microscopic characteristics (Table 4 and Fig. 2), all conidia had similar shapes (globose to subglobose, ellipsoidal), were smooth-walled, and their color varied from colorless to light or dark green. The sizes ranged from 1.67 × 1.51 to 0.76 × 0.78 µm. The shape of the phospholipids varied from pyramidal to longibrachiatum, and 3 to 4 verticillates were usually paired, with sizes ranging from 2.87–7.92 × 0.88–1.93 µm and terminal phialides up to 10 µm long. Based on both macro- and microcharacteristics, it can be concluded that the isolates belong to the genus *Trichoderma*. The spores, structures that produce spores and other characteristics of the *Trichoderma* isolates had similar morphologies. As a result, analyzing colony characteristics alone was not enough to identify the species. Consequently, accurate molecular identification is needed for species identification.

Molecular identification of *Trichoderma* spp.

PCR amplification, sequencing, and sequence analysis of the complete ITS 1 and 2 genes were used for identification of *Trichoderma* species. A single-

band image of the PCR products obtained is shown in Fig. (3). The PCR products had an approximate length of 640 bp for the ITS gene region and the results of DNA sequencing indicated that the fragments were similar in length and GC content (Table 5). However, further bioinformatics studies were performed where the nucleotide sequences of the ITS gene regions were compared via BLAST and the percentages of similarity were determined. Therefore, the isolates were identified as *T. harzianum*, *T. asperellum,* and *T. longibrachiatum*. The gene sequences for all the species were recorded in GenBank of NCBI and their corresponding accession numbers were retrieved (Table 5). The highest number of strains were identified as *T. harzianum* (23 strains), *T. asperellum* (sex strains), and finally *T. longibrachiatum* (two strains).

To compare the phylogenetic similarities among the 31 isolates, the phylogram included a strain of *T. reesei* from GenBank that served as a group species. The numbers displayed on the phylogenetic tree represent bootstrap values (Fig. 4). Upon observing the tree in Fig. (4), in the ITS phylogram, there were four clades in which *T. longibrachiatum* formed a separate clade, including two isolates; the *T. asperellum* clade included sex isolates; and the *T. harzianum* clade included 23 isolates. However, a separate clade included two isolates: one *T. asperellum* and the other *T. harzianum*.

Antagonistic assay

All the *Trichoderma* strains effectively suppressed *R. solani* growth (Fig. 5.a), among which the *T. asperellum* isolate MNF-NAH-Tricho5 presented the highest inhibition rate (71.43%), followed by the *T. harzianum* isolate MNF-NAH-Tricho30 (64.29%). The *T. longibrachiatum* isolate MNF-NAH-Tricho28 had the lowest inhibition rate (44.29%). In terms of the growth inhibition ability of *Trichoderma* spp. against *M. phaseolina,* the *T. harzianum* isolate MNF-NAH-Tricho30 presented the highest inhibition rate (85.13%), followed by *T. asperellum* MNF-NAH-Tricho5 (84.1%). *T. harzianum* MNF-NAH-Tricho4 presented the lowest inhibition rate (48.72%) (Fig. 5.b).

The *Trichoderma* isolates exhibited various strategies to combat phytopathogens, as illustrated in Fig. 6. During the antagonism tests against *R. solani* and *M. phaseolina*, the following observations were made, competition, antibiosis, or parasitism. The presence of a zone of inhibition and a change in culture media color indicate antibiosis, possibly caused by the secretion of secondary metabolites without direct contact with the mycelia. Among the isolates tested, seven isolates demonstrated antibiosis against *R. solani* (Fig. 6.1a), and eight isolates demonstrated antibiosis against *M. phaseolina* (Fig. 6.2a). The competition occurred when both fungi grew in the Petri dish until their mycelia intersected, at that moment, *Trichoderma* species started to create a barrier to suppress the pathogen spread.

This barrier strengthened over time, halting the advancement of the phytopathogen. This phenomenon was observed in seven isolates against *R. solani* (Fig. 6.1b) and 17 isolates against *M. phaseolina* (Fig. 6.2b). Mycoparasitism entails morphological modifications, including coiling and the formation of appressorium-like structures for host invasion. Among the 31 isolates, 16 exhibited mycoparasitism against *R. solani* (Fig. 6.1c), whereas only sex were exhibited against *M. phaseolina* (Fig. 6.2c). Microscopic examination (Fig. 6.3) revealed mycoparasitism, where *Trichoderma* hyphae were associated with phytopathogenic hyphae.

This research aimed to collect *Trichoderma* isolate samples from the root zones of various central Egyptian districts to identify the most effective ones for potential use as biocontrol agents (BCAs). This involved assessing their ability to produce chitinase and their capacity to combat *R. solani* and *M. phaseolina*. Given the significance of precise species identification in the process of selecting and validating microbial biological control agents, this study utilized a taxonomic approach derived from the combination of morphological and molecular characteristics (Shahid *et al*. 2014). This study utilized morphology-based identification to determine *Trichoderma* species, which is still considered a viable method for the identification of species (Anees *et al*. 2010). However, the initial identification of these isolates as *Trichoderma* solely based on the morphological characteristics of their colonies and microscopic observations was not sufficiently reliable to assign species, as some appeared to have been misidentified. The morphological identification of *Trichoderma* species is challenging for many researchers because of their significant structural similarities (Shahid *et al*. 2014). To achieve detailed molecular differentiation of the isolates, identification of the full ITS (ITS1 and ITS2) loci was employed. All the isolates were identified as *Trichoderma* spp., specifically *T. harzianum*, *T. longibrachiatum*, and *T. asperellum*. *T. harzianum* was the major species among these isolates, accounting for approximately 74% of the isolates, that was found primarily in the Delta of Egypt. The results were consistent with previous studies in this area, including those by El-Sobky *et al*. (2019 & 2024) and Hewedy *et al*. (2020). Furthermore, the current investigation demonstrated that the rhizospheres of various crops did not exhibit any substantial variation in the *Trichoderma* species communities. Hence, the limited diversity in this area may be attributed to biotic or abiotic variables, including plant species, soil physical and chemical features, microbial competition, and the application of fertilizers or pesticides in the area (Gupta *et al*. 2014). Furthermore, a visual representation of the genetic relationships among the isolates was generated through the creation of a phylogenetic tree. The ITS gene did not distinctly discriminate the *Trichoderma* strains into separate categories accurately, since two isolates were out of the three species clades. This may be due to the existence of non-

orthologous copies of the ITS genes within strains. Another possibility that there wasn't much sequence variation in the examined region or to the inherent stability of the ITS region in *Trichoderma* throughout evolutionary history. Previous research has highlighted the limitations of ITS sequences in defining *Trichoderma* strains (Chaverri *et al*. 2015). Also, the challenge of accurately differentiating species via the ITS region has been noted by many researchers (Balajee and Marr 2006). However, according to Druzhinina *et al*. (2005), the ITS region might help distinguish the *Trichoderma* genus from other closely related genera.

The effectiveness of the *Trichoderma* isolates was evaluated by testing their capability to compete with the pathogens *R. solani* and *M. phaseolina*. This involved observing the pathogen radial growth in the presence of *Trichoderma* strains and determining the degree of suppression in the pathogen growth induced by the *Trichoderma* strains. The results revealed that both pathogens were unable to resist the growth of the *Trichoderma* isolates. Specifically, the MNF-NAH-Tricho5 and MNF-NAH-Tricho30 isolates exhibited the greatest inhibition of both *Rhizoctonia solani* and *Macrophomina phaseolina*. The isolates of *Trichoderma* spp. exhibited antagonism, as evidenced by their efficiency in a significant mycelial growth inhibition of both *Rhizoctonia solani* and *Macrophomina phaseolina*. This confirms the occurrence of competition, antibiosis, and mycoparasitism phenomena previously reported for *Trichoderma* spp. (Hoitink *et al*. 2006). According to the findings of this study, the isolates MNF-NAH-Tricho5 and MNF-NAH-Tricho30 presented the highest potential among the *Trichoderma* isolates. The MNF-NAH-Tricho5 isolate exhibited antagonistic behavior via mycoparasitism against both pathogens. The mycoparasitic activity of the *Trichoderma* pathogen was shown through the coiling of its hyphae around the hyphae of the pathogenic fungus. In addition, the penetration of *Trichoderma* hyphae into other hyphae by the action of extracellular enzymes (e.g., chitinases and cellulases), which breakdown the fungal hyphae of phytopathogenic fungi, has been demonstrated as an additional method of mycoparasitic activity (Rajani *et al*. 2021). However, the MNF-NAH-Tricho30 isolate was antagonistic through competitive means.

CONCLUSION: This research provides comprehensive evaluation into the variety of *Trichoderma* species found in the root zone of crops in central Egypt. Through DNA sequence analysis, a successful species-level identification of thirty-one *Trichoderma* strains was achieved. *T. harzianum* was the most predominant species among the extracted strains, followed by *T. asperellum* and *T. longibrachiatum*. The MNF-NAH-Tricho5 and MNF-NAH-Tricho30 isolates exhibited strong antagonistic capabilities against two soil-borne pathogenic fungi, *Rhizoctonia solani* and *Macrophomina phaseolina*. To sum up, this study con-

firmed that the MNF-NAH-Tricho5 and MNF-NAH-Tricho30 isolates can potentially be used as biocontrol agents against *R. solani* and *M. phaseolina* in environmental applications.

SUMMARY

This research aimed to specifically identify 31 isolates at the species level using morphological characteristics combined with DNA barcoding sequence analysis of full-fragment rDNA ITS1 and ITS2 gene regions. The identified species were determined to be *T. harzianum* (23 strains), *T. asperellum* (6 strains), and *T. longibrachiatum* (2 strains). The phylogenetic analysis of the 31 isolates of the ITS region revealed that they formed four clades. Three of them included the isolates of each specific species, while a separate clade included two different isolates. The two isolates MNF-NAH-Tricho5 and MNF-NAH-Tricho30 presented the highest antifungal activity against *Rhizoctonia solani* (71.43 and 64.29%) and *Macrophomina phaseolina* (84.1 and 85.13%) according to the dual culture assay. Finally, various strategies to combat phytopathogens, including competition, antibiosis, or parasitism, have been developed for *Trichoderma* isolates. The overall study confirmed that the MNF-NAH-Tricho5 and MNF-NAH-Tricho30 strains may serve as prospective biocontrol agents to combat *Rhizoctonia solani* and *Macrophomina phaseolina* in environmental applications.

REFERENCES

Anees M., Tronsmo A., Edel-Hermann V., Hjeljord L., Héraud C. and Steinberg C., (2010). Characterization of field isolates of *Trichoderma* antagonistic against *Rhizoctonia solani*. Fungal Biol., 114:691-701. https:// doi.org/ 10. 1016 /J. FUNBIO. 2010.05.007.

Balajee S. A. and Marr K. A., (2006). Phenotypic and genotypic identification of human pathogenic aspergilli. Future Microbiol, 1:435-445. https://doi.org/10.2217/17460913. 1.4.435 .

Cai F. and Druzhinina I. S., (2021). In honor of John Bissett: authoritative guidelines on molecular identification of *Trichoderma*. Fungal Divers 107:1-69. https://doi.org/10. 1007 /S13225-020-00464-4 .

Chaverri P., Branco-Rocha F., Jaklitsch W., Gazis R., Degenkolb T. and Samuels G., (2015). Systematics of the *Trichoderma harzianum* species complex and the re-identification of commercial biocontrol strains. Mycologia, 107 :558-590. https://doi.org/ 10.3852 /14-147.

Dhingra O. D. and Sinclair J. B., (1995). Basic Plant Pathology Methods (2nd ed.). CRC Press. 1-434. https: //doi.org/10.1201/9781315138138

Druzhinina I. S., Kopchinskiy A. G., Komoń M., Bissett J., Szakacs G. and Kubicek C. P., (2005). An oligonucleotide barcode for species identification in *Trichoderma* and *Hypocrea*. Fungal Genet. Biol., 42:813-828. https://doi.org/10.1016/J.FGB.2005.06.007.

Edgar R. C., (2004). MUSCLE: multiple sequence alignment with high accuracy and high throughput. Nucleic Acids Res., 32:1792-1797. https://doi.org/10.1093/NAR/GKH340 .

Elad Y., (2000). Biological control of foliar pathogens by means of *Trichoderma harzianum* and potential modes of action. Crop Protection, 19:709-714. https://doi.org/101016/S0261-2194(00)00094-6.

Elhamouly N., Hewedy O., Zaitoon A., Miraples A., Elshorbagy O., Hussien S., El-Tahan A. and Peng D., (2022). The hidden power of secondary metabolites in plant-fungi interactions and sustainable phytoremediation. *Front. Plant Sci.*, 13:1044896. doi: 10.3389/fpls.2022.1044896.

El-Hasan A., Walker F., Klaiber I., Schöne J., Pfannstiel J. and Voegele R. T., (2022). New approaches to manage Asian soybean rust (*Phakopsora pachyrhizi*) using *Trichoderma* spp. or their antifungal secondary metabolites. Meta 12:507. https://doi: 10.3390/metabo12060507

El-Sobky M., Fahmi A., Eissa R. and El-Zanaty A., (2019). Genetic Characterization of *Trichoderma* spp. Isolated from Different Locations of Menoufia, Egypt and Assessment of their Antagonistic Ability. J. Microb Biochem. Technol., 11(1):409. https://doi.org/10.4172/1948-5948.1000409.

El-Sobky M. A., Eissa R. A., Abdel-Lateif K. S., Fahmi A. I., El-Zanaty A. M., Hassan M. M. and ElSharkawy M, M., (2024). Genetic diversity assessment of *Trichoderma* spp. isolated from various Egyptian locations using its gene sequencing marker, rep-PCR, and their cellulolytic activity. Egypt. J. Biol. Pest. Control., 34:1-10. https://doi.org/10.1186/S41938-024-00784-6.

Fahmi A. I., Eissa R. A., El-Halfawi K. A., Hamza H. A. and Helwa M. S., (2016). Identification of *Trichoderma* spp. by DNA Barcode and Screening for Cellulolytic Activity. J Microb. Biochem. Technol., 8:202-209. https://doi.org/10.4172/1948-5948.1000286.

Ghasemi S., Safaie N., Shahbazi S., Shams-Bakhsh M. and Askari H., (2019). Enhancement of Lytic Enzymes Activity and Antagonistic Traits of *Trichoderma harzianum* Using γ-Radiation Induced Muta-

tion. J. Agr. Sci. Tech., 21(4):1035-1048.

Gupta V., Schmoll M., Herrera-Estrella A., Upadhyay R., Druzhinina I. and Tuohy M., (eds) (2014). Biotechnology and Biology of *Trichoderma*. Biotechnology and Biology of *Trichoderma*, Elsevier, 1-549. https://doi.org/10.1016/ C2012-0-00434-6.

Hall T., Biosciences I. and Carlsbad C., (2011). BioEdit: An important software for molecular biology. GERF Bulletin of Biosciences, 2(1):60-61.

Hermosa M., Grondona I., Iturriaga E., Diaz-Minguez J., Castro C., Monte E. and Garcia-Acha I., (2000). Molecular Characterization and Identification of Biocontrol Isolates of *Trichoderma* spp. Appl. Environ. Microbiol., 66 (5) :1890-1898 https://doi.org/10.1128/AEM.66.5. 1890-1898.2000 .

Hewedy O., Abdel Lateif K., Seleiman M., Shami A., Albarakaty F. and El-Meihy R., (2020). Phylogenetic Diversity of *Trichoderma* Strains and Their Antagonistic Potential against Soil-Borne Pathogens under Stress Conditions. Biology, 9(8):189. https://doi.org/10.3390 /BIOLOGY9080189.

Hoitink H. A. J., Madden L. V. and Dorrance A. E., (2006). Systemic resistance induced by *Trichoderma* spp.: Interactions between the Host, the Pathogen, the Biocontrol Agent, and Soil Organic Matter Quality. Phytopathology, 96 (2): 186-189. https://doi.org/ 10.1094/PHYTO-96-0186.

Kredics L., Büchner R., Balázs D., Allaga H., Kedves O., Racić G., Varga A., Nagy V., Vágvölgyi C. and Sipos G., (2024). Recent advances in the use of *Trichoderma*-containing multicomponent microbial inoculants for pathogen control and plant growth promotion. World J. Microbiol Biotechnol., 40(5):1-14. https://doi.org/10.1007/S11274-024-03965-5.

Lahlali R., Ezrari S., Radouane N., Kenfaoui J., Esmaeel Q., El Hamss H, Belabess Z. and Barka E. A., (2022). Biological Control of Plant Pathogens: A Global Perspective. Microorganisms, 10(3):596 https: //doi.org/10.3390/MICROORGANISMS10030596.

Mukherjee P. K., Mendoza-Mendoza A., Zeilinger S. and Horwitz B. A., (2022). Mycoparasitism as a mechanism of *Trichoderma*-mediated suppression of plant diseases. Fungal Biol. Rev., 39:15-33. https://doi.org/10.1016/J.FBR. 2021.11.004.

Raja H. A., Miller A. N., Pearce C. J. and Oberlies N. H., (2017). Fungal identification using molecular tools: a primer for the natural

products. Research Community. J Nat Prod., 80(3):756-770. https://doi.org/10.1021/ACS.JNATPROD.6B01085.

Rajani P., Rajasekaran C., Vasanthakumari M. M., Olsson S. B., Ravikanth G. and Uma Shaanker R., (2021). Inhibition of plant pathogenic fungi by endophytic *Trichoderma* spp. through mycoparasitism and volatile organic compounds. Microbiol Res., 242:126595 https://doi.org/10.1016/J.MICRES.2020.126595.

Riffiani R., Wada T., Shimomura N., Yamaguch T. and Aimi T., (2021). An optimized method for high-quality DNA extraction medicinal fungi *Mycoleptodonoides aitchisonii* for whole genome sequencing. IOP Conf. Ser Earth Environ. Sci., 948(1):012032. https://doi.org/10.1088/1755-1315/948/1/012032.

Sequencher® version 5.4.6 DNA sequence analysis software, Gene Codes Corporation, Ann Arbor, MI USA http://www.g enecodes.com.

Shahid M., Srivastava M., Kumar V., Singh A., Sharma A., Pandey S., Rastogi S., Pathak N. and Srivastava A. K., (2014). Phylogenetic diversity analysis of *Trichoderma* species based on internal transcribed spacer (ITS) marker. Afr. J. Biotechnol., 13(3):449-455. https://doi.org/10.5897/AJB2013.13075.

Tamura K., Stecher G. and Kumar S., (2021). MEGA11: Molecular Evolutionary Genetics Analysis Version 11. Mol. Biol. Evol., 38(7):3022-3027. https://doi. Org /10.1093/MOLBEV/MSAB120.

Yadav M., Dubey M. K. and Upadhyay R. S., (2021). Systemic Resistance in Chilli Pepper against Anthracnose (Caused by *Colletotrichum truncatum*) Induced by *Trichoderma harzianum*, *Trichoderma asperellum* and *Paenibacillus dendritiformis*. J. Fungi, 7(4):307 https://doi.org/10.3390/JOF7040307.

Table (1): PCR Primer sequences used in *Trichoderma* molecular identification (Cai and Druzhinina, 2021).

Primer name	Sequence (5'-3')	Target
ITS5	GGAAGTAAAAGTCGTAACAAGG	ITS, including the 5.8S rRNA
ITS4	TCCTCCGCTTATTGATATGC	

Table (2): PCR amplification program.

Target	Initial denaturation	35 cycles			Final extension
ITS	95°C - 5 minutes	Denaturation 95°C - 15 seconds	Annealing 56°C – 15 seconds	Extension 72°C - 1 minute	72°C - 5 minute

Table (3): Macroscopic Examination: Colony characters of *Trichoderma* isolates grown on SNA for 5 days at 25°C with alternating 12 h light and 12 h darkness.

Trichoderma isolate number	Shape	Color	Reverse color	Concentric rings Number	Edge
T.1	Circular	Green	Light yellow	3	Smooth
T.2	Circular	Dark green	No color	3	Smooth
T.3	Circular	Dark green	No color	2	Smooth
T.4	Circular	Green	Light amber	3	Smooth
T.5	Circular	Dark green	White	3	Smooth
T.6	Serrate	Light/dark green with	No color	3	Wavey
T.7	Circular	Green	No color	1	Smooth
T.8	Circular	Light/dark green	White	3	Smooth
T.9	Circular	Light/dark green	White	3	Smooth
T.10	Circular	Dark green	White	2	Smooth
T.11	Circular	Light green with white	Light yellow	1	Smooth
T.12	Serrate	Light/dark green with	Creamy	3	Wavey
T.13	Circular	Dark green	White	3	Smooth
T.14	Circular	Green	Yellow	1	Smooth
T.15	Circular	Light/dark green	Light amber	2	Smooth
T.16	Serrate	White/green	Amber	1	Wavey
T.17	Circular	Green	No color	No Concentric rings	Smooth
T.18	Circular	Green/Light green	No color	3	Smooth
T.19	Circular	Dark green surrounded	No color	No Concentric rings	Smooth
T.20	Serrate	Light/dark green with	Creamy/Light yellow	1	Wavey
T.21	Serrate	yellowish white	Amber	No Concentric rings	Wavey
T.22	Circular	Green	No color	2	Smooth
T.23	Serrate	White	Amber	No Concentric rings	Wavey
T.24	Circular	Dark green	White	3	Smooth
T.25	Serrate	Yellow	Amber	No Concentric rings	Wavey
T.26	Circular	Green with some vel-	No color	3	Smooth
T.27	Circular	Dark green	No color	2	Smooth
T.28	Circular	Dark green surrounded	No color	No Concentric rings	Smooth
T.29	Circular	Light/dark green	Light amber	2	Smooth
T.30	Circular	Green	No color	No Concentric rings	Smooth
T.31	Serrate	Dark green	No color	2	Wavey

Table (4): Microscopic examination: Conidia and Phialides characteristics of *Trichoderma* isolates grown on SNA after one week at 25°C under a regimen of alternating 12 h light and 12 h darkness.

Trichoderma isolate number	Conidia				Phialides		
	*Average Length (µm)	*Average Width (µm)	Color	Shape	*Average Length (µm)	*Average Width (µm)	Branching pattern
T.1	1.30	1.24	Dark green	Globose	3.16	1.64	Pyramidal
T.2	1.07	1.02	Colorless	Globose	3.97	1.31	Pyramidal
T.3	1.09	0.90	Green	Sub globose	2.88	1.47	Pyramidal
T.4	1.18	0.98	Light green	Sub globose	3.55	1.82	Pyramidal
T.5	1.45	1.20	Light green	Sub globose to	4.16	1.56	Pyramidal
T.6	1.00	0.86	Green	Sub globose	3.70	1.63	Pyramidal
T.7	1.45	1.26	Dark green	Sub globose to	2.87	1.73	Pyramidal
T.8	1.43	1.22	Light green	Sub globose to	5.34	1.63	Pyramidal
T.9	1.51	1.51	Light green	Globose	5.38	1.37	Pyramidal
T.10	1.06	1.07	Light green	Globose	3.73	1.65	Pyramidal
T.11	0.99	1.13	Green	Sub globose	3.65	1.08	Pyramidal
T.12	0.92	0.92	Green	Globose	4.14	1.64	Pyramidal
T.13	1.02	1.30	Light green	Sub globose to	7.92	1.63	Pyramidal
T.14	0.92	0.89	Green	Globose	5.13	1.93	Pyramidal
T.15	1.07	0.98	Light green	Globose	3.35	1.74	Pyramidal
T.16	1.09	1.07	Green	Globose	5.00	1.59	Pyramidal
T.17	1.33	1.37	Colorless	Globose	5.76	1.14	Pyramidal
T.18	1.26	1.22	Light green	Globose	5.38	1.62	Pyramidal
T.19	1.67	1.11	Dark green	Ellipsoidal	4.50	1.20	Longibrachiatum
T.20	1.00	0.88	Green	Sub globose	3.37	1.56	Pyramidal
T.21	0.90	0.94	Colorless	Globose	5.07	1.49	Pyramidal
T.22	1.19	1.19	Green	Globose	3.26	1.27	Pyramidal
T.23	0.96	0.93	Colorless	Globose	4.02	1.57	Pyramidal
T.24	1.13	1.21	Light green	Globose	4.69	1.73	Pyramidal
T.25	0.76	0.78	Light green	Globose	3.77	1.40	Pyramidal
T.26	1.07	1.07	Green	Globose	4.26	1.56	Pyramidal
T.27	1.06	0.98	Green	Globose	4.50	1.66	Pyramidal
T.28	1.27	1.52	Dark green	Sub globose to	4.44	0.88	Longibrachiatum
T.29	1.09	1.01	Green	Globose	3.54	1.61	Pyramidal
T.30	1.06	0.96	Light green	Globose	4.69	1.21	Pyramidal
T.31	0.81	0.90	Green	Globose	4.53	1.65	Pyramidal

*Average length of 5-10 Conidia or Phialides. *Average width of 5-10 Conidia or Phialides

Table (5): Molecular identification of *Trichoderma* isolates based on ITS region.

Isolates Code	Alignments Description	E value	Identity %	NCBI GenBank accession number	Species name	Sequence length (bp)	GC content %
MNF-NAH-	*Trichoderma harzianum* isolate T13	0.0	100	OR944917	*Trichoderma har-*	530	56
MNF-NAH-	*Trichoderma harzianum* isolate SO-	0.0	99.81	OR944911	*Trichoderma har-*	529	56.1
MNF-NAH-	*Trichoderma harzianum* isolate	0.0	99.43	OR944910	*Trichoderma har-*	527	56.4
MNF-NAH-	*Trichoderma harzianum* isolate	0.0	100	OR944925	*Trichoderma har-*	529	55.8
MNF-NAH-	*Trichoderma asperellum* isolate	0.0	100	OR944900	*Trichoderma*	515	55.7
MNF-NAH-	*Trichoderma harzianum* strain	0.0	100	OR944921	*Trichoderma har-*	523	56.4
MNF-NAH-	*Trichoderma harzianum* clone	0.0	100	OR944922	*Trichoderma har-*	531	55.9
MNF-NAH-	*Trichoderma asperellum* isolate	0.0	100	OR944899	*Trichoderma*	515	55.7
MNF-NAH-	*Trichoderma asperellum* isolate	0.0	100	OR944898	*Trichoderma*	515	55.7
MNF-NAH-	*Trichoderma harzianum* strain 7-5	0.0	100	OR944913	*Trichoderma har-*	531	55.9
MNF-NAH-	*Trichoderma harzianum* isolate	0.0	100	OR944914	*Trichoderma har-*	532	55.8
MNF-NAH-	*Trichoderma harzianum* isolate	0.0	100	OR944915	*Trichoderma har-*	530	55.8
MNF-NAH-	*Trichoderma asperellum* isolate	0.0	100	OR944897	*Trichoderma*	567	55.7
MNF-NAH-	*Trichoderma harzianum* isolate H1	0.0	100	OR944916	*Trichoderma har-*	532	55.8
MNF-NAH-	*Trichoderma harzianum* strain T28	0.0	99.81	OR944907	*Trichoderma har-*	530	56
MNF-NAH-	*Trichoderma harzianum* isolate	0.0	99.81	OR944905	*Trichoderma har-*	532	55.5
MNF-NAH-	*Trichoderma harzianum* isolate	0.0	99.81	OR944924	*Trichoderma har-*	531	56.2
MNF-NAH-	*Trichoderma asperellum* isolate TZ	0.0	99.81	OR944901	*Trichoderma*	515	55.7
MNF-NAH-	*Trichoderma longibrachiatum*	0.0	100	OR944903	*Trichoderma*	550	57.8
MNF-NAH-	*Trichoderma harzianum* isolate	0.0	100	OR944918	*Trichoderma har-*	532	55.8
MNF-NAH-	*Trichoderma harzianum* strain	0.0	100	OR944919	*Trichoderma har-*	530	56
MNF-NAH-	*Trichoderma harzianum* isolate	0.0	100	OR944920	*Trichoderma har-*	530	56
MNF-NAH-	*Trichoderma harzianum* clone	0.0	100	OR944896	*Trichoderma har-*	576	55.9
MNF-NAH-	*Trichoderma asperellum* strain T19	0.0	100	OR944902	*Trichoderma*	514	55.8
MNF-NAH-	*Trichoderma harzianum* isolate	0.0	99.81	OR944926	*Trichoderma har-*	528	56.3
MNF-NAH-	*Trichoderma harzianum* strain	0.0	99.62	OR944923	*Trichoderma har-*	529	56
MNF-NAH-	*Trichoderma harzianum* BW6	0.0	98.65	OR944909	*Trichoderma har-*	517	56.1
MNF-NAH-	*Trichoderma longibrachiatum* iso-	0.0	100	OR944904	*Trichoderma*	550	57.8
MNF-NAH-	*Trichoderma harzianum* isolate 112	0.0	99.81	OR944906	*Trichoderma har-*	528	56.3
MNF-NAH-	*Trichoderma harzianum* isolate	0.0	99.81	OR944908	*Trichoderma har-*	531	55.9
MNF-NAH-	*Trichoderma harzianum* strain	0.0	99.91	OR944912	*Trichoderma har-*	530	56

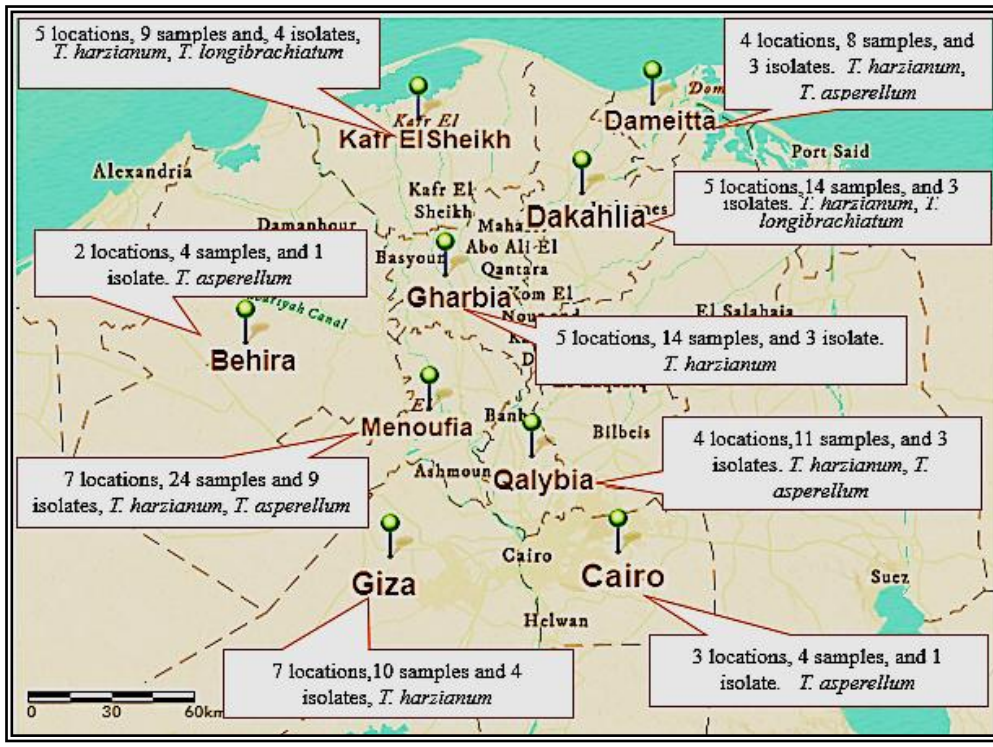

Fig. (1). Illustrative map of Central Egypt governorates with locations, collected samples, isolates obtained from each site, and *Trichoderma* species found.

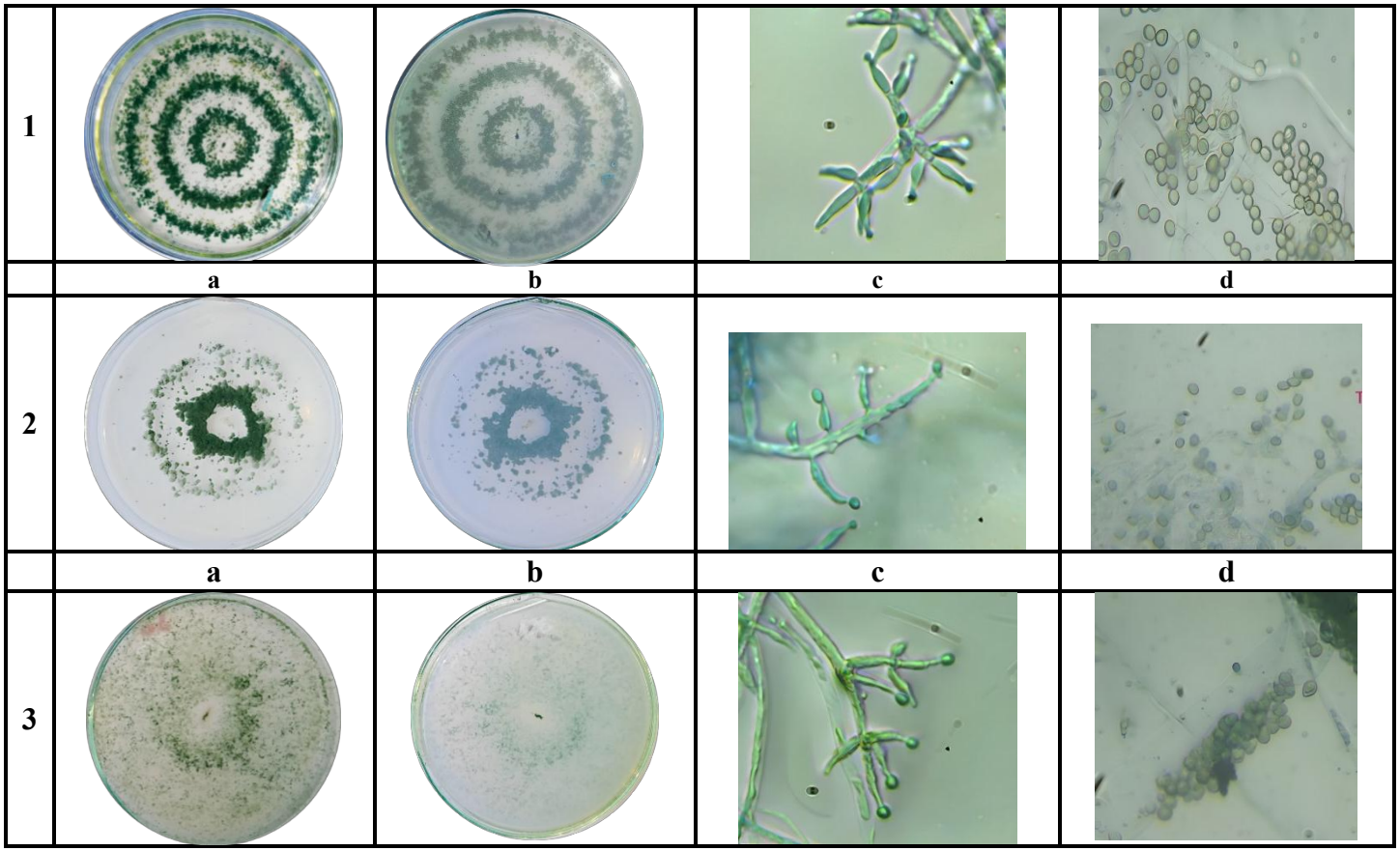

Fig. (2). Morphological identification on SNA media after 7 days of: 1 *Trichoderma asperellum*, 1a Colony growth, 1b Reverse colo the plate, 1c Phialides shape and branching pattern, 1d Conidia shape and size. 2 *Trichoderma longibrachiatum*, 2a Col growth, 2b Reverse color of the plate, 2c Phialides shape and branching pattern, 2d Conidia shape and size. 3 *Trichoderma l zianum*, 3a Colony growth, 3b Reverse color of the plate, 3c Phialides shape and branching pattern, 3d Conidia shape and size

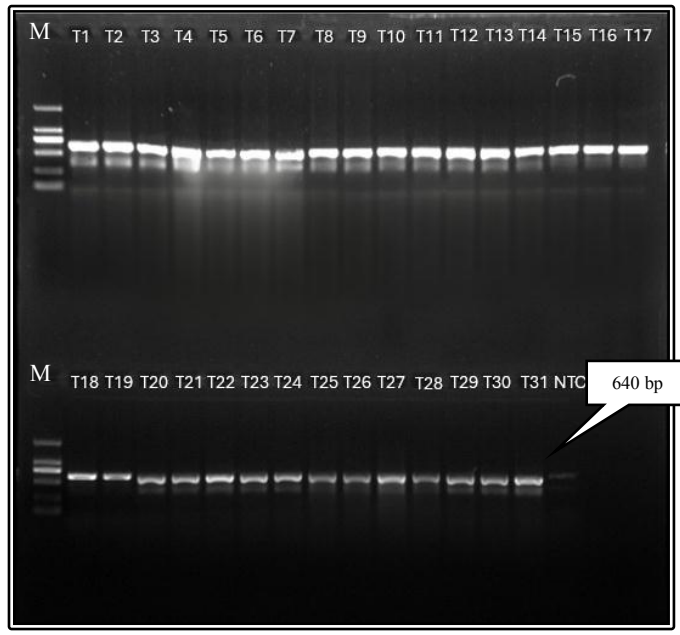

Fig. (3). Full ITS 1 and 2 regions PCR products of 31 *Trichoderma* isolates, M: 100-2000 bp DNA molecular ladder.

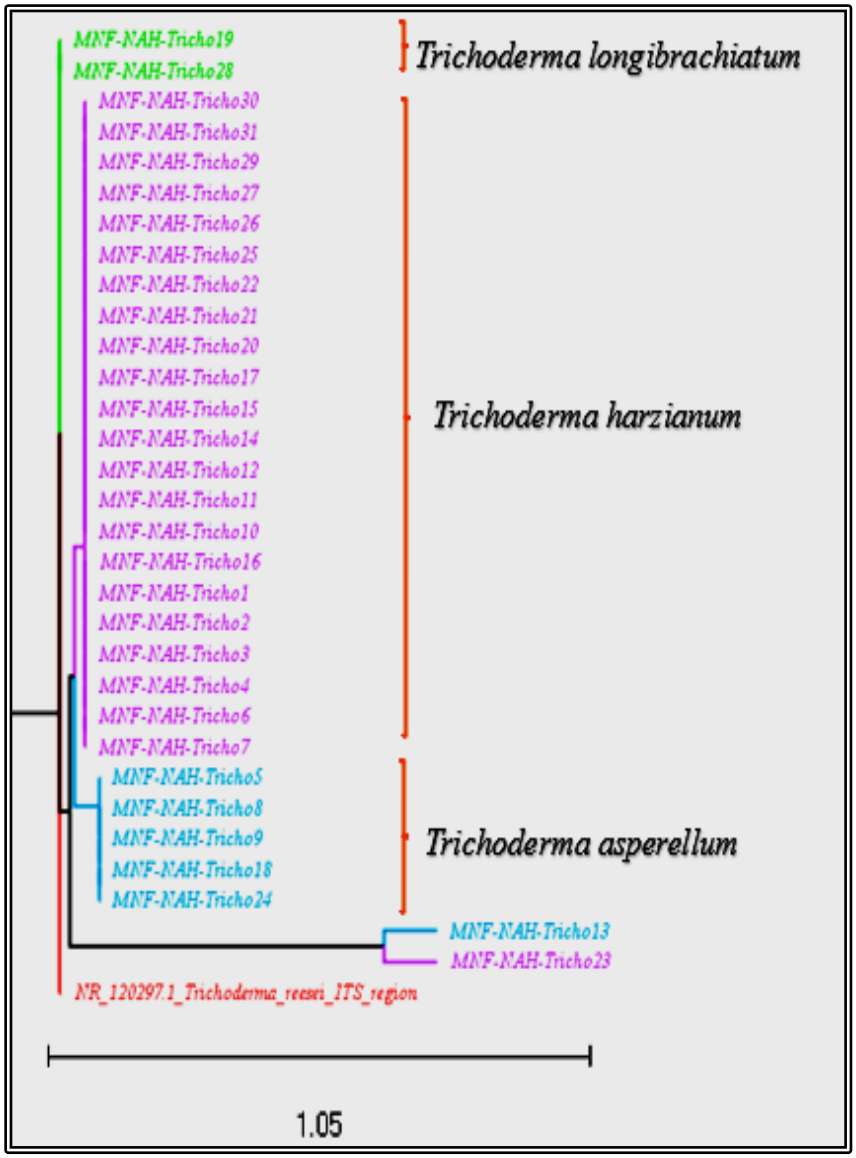

Fig. (4). Phylogenetic tree revealing the genetic diversity of *Trichoderma* isolates based on the DNA sequences of ITS region, and *Trichoderma reesei* served as outgroup strain. The numbers above the branches are bootstrap values obtained with 1000 bootstraps. The scale bar indicates the number of nucleotide changes. The type species and bootstrap-supported clades are in different colors.

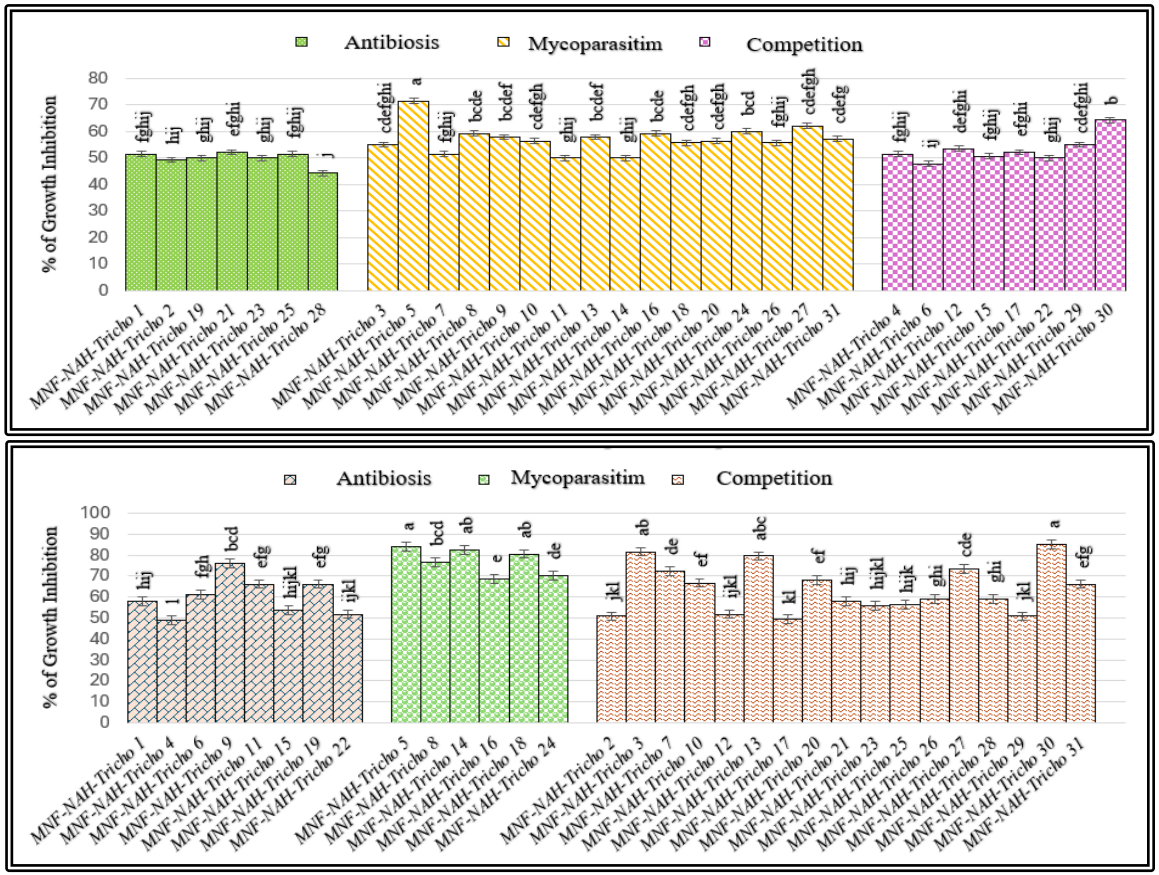

Fig. (5). *In vitro* antagonistic effect of 31 *Trichoderma* isolates against **a** *Rhizoctonia solani*, and **b** *Macrophomina phaseolina*, after 7 days of inoculation using dual culture assay. Superscript letters indicate Duncan's grouping means with the same letter are not significantly different.

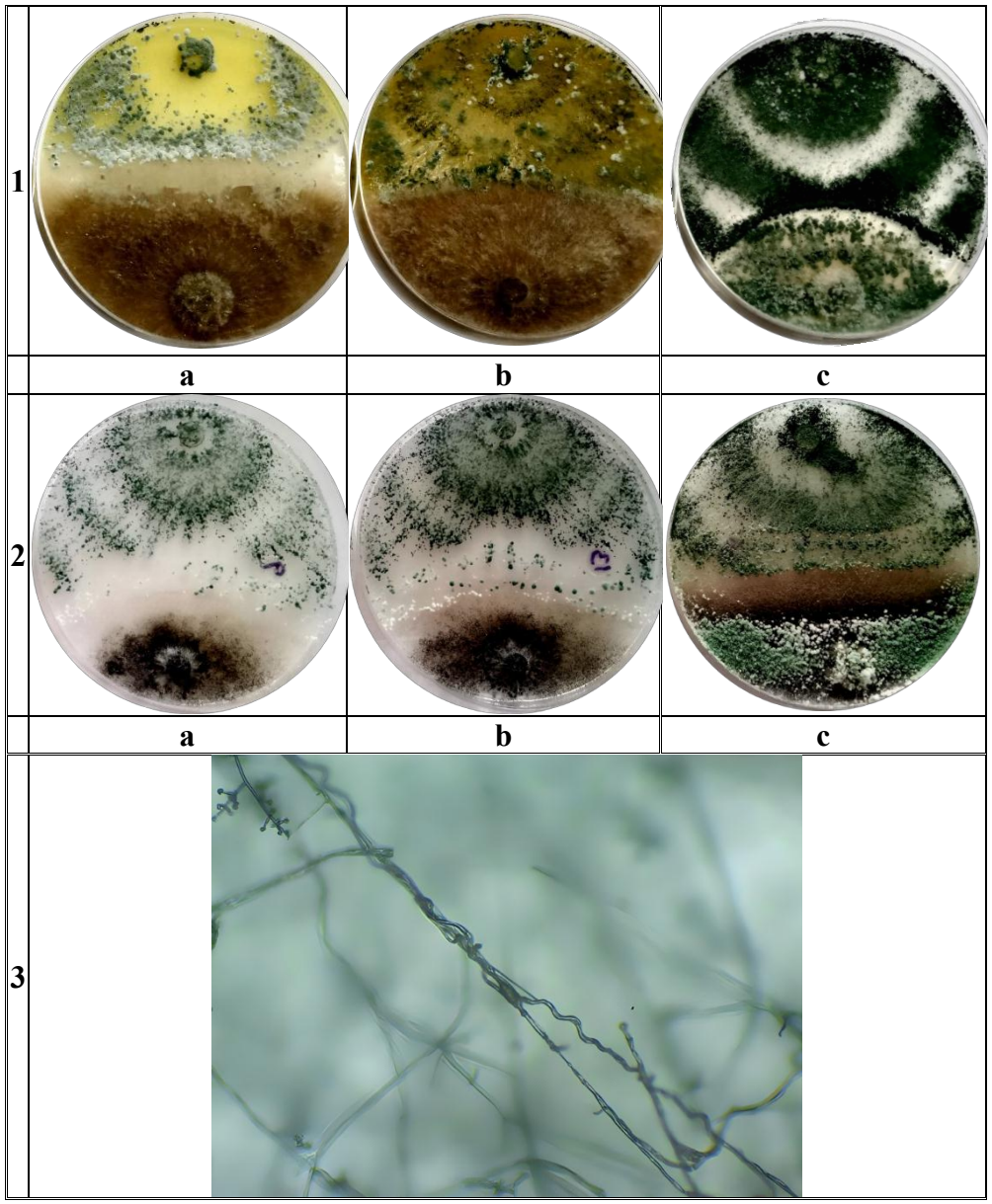

Fig. (6). *Trichoderma* mechanisms of inhibition of: 1 *Rhizoctonia solani*, a Antibiosis, b Competition, c Mycoparasitism, 2 *Macrophomina phaseolina* a Antibiosis, b Competition, c Mycoparasitism. 3 Coiling of *Trichoderma*'s hyphae around *Macrophomina phaseolina*'s hypha.